

Effect of the Presence of a Heat Conducting Horizontal Square Block on Mixed Convection inside a Vented Square Cavity

Md. M. Rahman¹, M. A. Alim¹, S. Saha², M. K. Chowdhury¹

¹Department of Mathematics
Bangladesh University of Engineering and Technology (BUET)
Dhaka-1000, Bangladesh
mmustafizurrahman@math.buet.ac.bd

²Department of Mechanical Engineering
The University of Melbourne
Victoria 3010, Australia

Received: 2009-03-16 **Revised:** 2009-08-15 **Published online:** 2009-11-11

Abstract. Finite element method is used to solve two-dimensional governing mass, momentum and energy equations for steady state, mixed convection problem inside a vented square cavity. The cavity consists of adiabatic left, top and bottom walls and heated right vertical wall; but it also contains a heat conducting horizontal square block located somewhere inside the cavity. Forced flow conditions are imposed by providing an inlet at the bottom of the left wall and an exit at the top of the right wall, through which the working fluid escape out of the cavity. The aim of the study is to describe the effect of such block on the flow and thermal fields. The investigations are conducted for various values of geometric size, location and thermal conductivity of the block under constant Reynolds and Prandtl numbers. Various results such as the streamlines, isotherms, heat transfer rates in terms of the average Nusselt number, average fluid temperature in the cavity and the temperature at the center of solid block are presented for different parameters. It is observed that the block size and location have significant effect on both the flow and thermal fields but the solid-fluid thermal conductivity ratio has insignificant effect on the flow field. The results also indicate that the average Nusselt number at the heated surface, the average temperature of the fluid inside the cavity and the temperature at the center of solid block are strongly dependent on the configurations of the system studied under different geometrical and physical conditions.

Keywords: finite element method, square block, vented cavity and mixed convection.

Nomenclature

d	dimensional length of the block [m]	g	gravitational acceleration [ms^{-2}]
D	dimensionless length of the block	h	convective heat transfer coefficient

k	thermal conductivity of fluid [Wm ⁻¹ K ⁻¹]	p	dimensional pressure [Nm ⁻²]
k_s	thermal conductivity of the solid block [Wm ⁻¹ K ⁻¹]	P	dimensionless pressure
K	solid fluid thermal conductivity ratio	Pr	Prandtl number
L	length of the cavity [m]	Ra	Rayleigh number
l_x	dimensional distance between y -axis and the block center [m]	Re	Reynolds number
l_y	dimensional distance between x -axis and the block center [m]	Ri	Richardson number
L_x	dimensionless distance between y -axis and the block center	T	dimensional temperature [K]
L_y	dimensionless distance between x -axis and the block center	u, v	dimensional velocity components [ms ⁻¹]
Nu	average Nusselt number	U, V	dimensionless velocity components
		\bar{V}	cavity volume [m ³]
		w	height of the opening [m]
		x, y	Cartesian coordinates [m]
		X, Y	dimensionless Cartesian coordinates

Greek symbols

α	thermal diffusivity [m ² s ⁻¹]
β	thermal expansion coefficient [K ⁻¹]
ν	kinematic viscosity [m ² s ⁻¹]
θ	dimensionless temperature
ρ	density of the fluid [kgm ⁻³]

Subscripts

av	average
h	heated wall
i	inlet state
c	block center
s	solid

Abbreviation

CBC convective boundary conditions

1 Introduction

Efficient convection heat transfers are essential in modern technology and also very important in many industrial areas. Hence, it is necessary to study and simulate these phenomena. Several numerical and experimental methods have been developed to investigate cavities with and without obstacle because these geometries have practical engineering and industrial applications, such as in the design of solar collectors, thermal design of building, air conditioning, cooling of electronic devices, furnaces, lubrication technologies, chemical processing equipment, drying technologies etc. Analysis of above phenomena, incorporating a solid heat conducting obstruction extends its usability to practical situations. Particularly, a conductive material in an inert atmosphere inside a furnace with a constant flow of gas from outside and the cooling of electronic circuit boards constitutes some practical applications for the present study. Conjugate natural convection heat transfer inside an inclined square cavity with an internal conducting block was studied by Das and Reddy [1]. At the same time, Zhao et al. [2] numerically investigated conjugate natural convection in enclosures with external and internal heat

sources and Xu et al. [3] experimentally observed the thermal flow around a square obstruction on a vertical wall in a differentially heated cavity. Later on, Bhoite et al. [4] performed numerical investigation on the problem of mixed convection flow and heat transfer in a shallow enclosure with a series of block-like heat generating components for a range of Reynolds and Grashof numbers and block-to-fluid thermal conductivity ratios. They showed that higher Reynolds numbers created a recirculation of increasing strength at the core region and the effect of buoyancy became insignificant beyond a Reynolds number of typically 600 and hence the thermal conductivity ratio had a negligible effect on the velocity fields. Braga and de Lemos [5] investigated steady laminar natural convection within a square cavity filled with a fixed volume of conducting solid material consisting of either circular or square obstacles. They used finite volume method with a collocated grid to solve governing equations. They found that the average Nusselt number for cylindrical rods was slightly lower than those for square rods. The problem of laminar natural convection heat transfer in a square cavity with an adiabatic arc shaped baffle was numerically analyzed by Tasnim and Collins [6]. They identified that flow and thermal fields were modified by the blockage effect of the baffle and the degree of flow modification due to blockage was enhanced by increasing the shape parameter of the baffle. Bilgen and Yamane [7] examined the effect of conjugate heat transfer by laminar natural convection and conduction in two-dimensional rectangular enclosures with openings. A chimney inside the enclosure was simulated as a vertical rectangular body with a uniform heat flux on one side and insulation on the other. They investigated the effects of the various geometrical parameters and the thickness of the insulation layer on the fluid flow and heat transfer characteristics. Dong and Li [8] studied conjugate effect of natural convection and conduction in a complicated enclosure. They observed the influences of material character, geometrical shape and Rayleigh number on the heat transfer in the overall concerned region. They finally concluded that the flow and heat transfer increased with the increase of thermal conductivity in the solid region and besides, both geometric shape and Rayleigh number also affected the overall flow and heat transfer greatly. Roychowdhury et al. [9] analyzed the natural convective flow and heat transfer features for a heated cylinder placed in a square enclosure with different thermal boundary conditions. House et al. [10] studied the effect of a centered, square, heat conducting body on natural convection in a vertical enclosure. They showed that heat transfer across the cavity enhanced or reduced by a body with a thermal conductivity ratio less or greater than unity. The same geometry was considered in the numerical study of Oh et al. [11], where the conducting body generated heat within the cavity. Under these situations, it was shown that the flow was driven by a temperature difference across the cavity and a temperature difference caused by the heat-generating source. Very recently Rahman et al. [12] analyzed mixed convection in a rectangular cavity with a heat conducting horizontal circular cylinder by using finite element method.

In the light of the above literature, it has been pointed out that there is no significant information about mixed convection processes when a heat conducting square block exists within a vented cavity in different locations. The purpose of the present study is to examine how the size, location and thermal conductivity of the inner heat-conducting block affect the mixed convection phenomena within the vented cavity.

2 Problem definition

A schematic diagram of the system considered in the present study is shown in Fig. 1. The system consists of a square cavity with sides of length L , within which a square heat conducting block with length d and thermal conductivity k_s is located somewhere (l_x, l_y) within the cavity. A Cartesian co-ordinate system is used with origin at the lower left corner of the computational domain. The top, bottom and left vertical walls of the cavity are kept adiabatic and the right vertical wall is kept at a uniform constant temperature, T_h . The inflow opening located on the bottom of the left wall and the outflow opening of the same size is placed at the top of the opposite heated wall as shown in Fig. 1. For simplicity, the size of the two openings, w is set equal to the one-tenth of the cavity length (L). Cold air flows through the inlet inside the cavity at a uniform velocity, u_i . It is also assumed that the incoming flow is at the ambient temperature T_i and the outgoing flow is assumed to have zero diffusion flux for all dependent variables i.e. convective boundary conditions (CBC). All solid boundaries are assumed to be rigid no-slip walls. Emphasis is placed on the effect of the various orientations and dimension of the heat-conducting block.

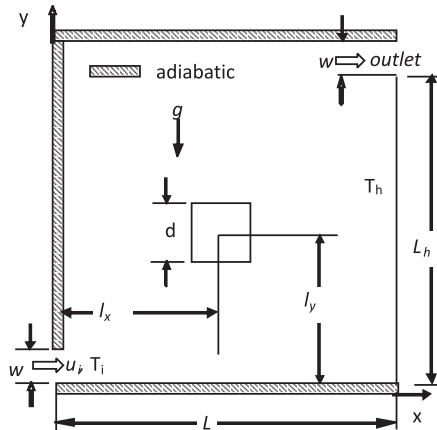


Fig. 1. Schematic of the problem with the domain and boundary conditions.

3 Mathematical model

In the present problem, it can be considered that the flow is steady, two-dimensional, laminar incompressible and there is no viscous dissipation. The gravity acts in the vertically downward direction, fluid properties are constant and fluid density variations are neglected except in the buoyancy term (Boussinesq approximation) and radiation effect is neglected.

Using non-dimensional variables defined below, the non-dimensional forms of the

governing equations of the present problem are obtained as follows:

$$\frac{\partial U}{\partial X} + \frac{\partial V}{\partial Y} = 0, \quad (1)$$

$$U \frac{\partial U}{\partial X} + V \frac{\partial U}{\partial Y} = -\frac{\partial P}{\partial X} + \frac{1}{Re} \left(\frac{\partial^2 U}{\partial X^2} + \frac{\partial^2 U}{\partial Y^2} \right), \quad (2)$$

$$U \frac{\partial V}{\partial X} + V \frac{\partial V}{\partial Y} = -\frac{\partial P}{\partial Y} + \frac{1}{Re} \left(\frac{\partial^2 V}{\partial X^2} + \frac{\partial^2 V}{\partial Y^2} \right) + Ri \theta, \quad (3)$$

$$U \frac{\partial \theta}{\partial X} + V \frac{\partial \theta}{\partial Y} = \frac{1}{Re Pr} \left(\frac{\partial^2 \theta}{\partial X^2} + \frac{\partial^2 \theta}{\partial Y^2} \right), \quad (4)$$

For heat conducting block, the energy equation is

$$\frac{\partial^2 \theta_s}{\partial X^2} + \frac{\partial^2 \theta_s}{\partial Y^2} = 0. \quad (5)$$

The non-dimensional variables used in the above equations are defined as

$$\begin{aligned} X &= \frac{x}{L}, & Y &= \frac{y}{L}, & U &= \frac{u}{u_i}, & V &= \frac{v}{u_i}, \\ P &= \frac{p}{\rho u_i^2}, & D &= \frac{d}{L}, & L_x &= \frac{l_x}{L}, & L_y &= \frac{l_y}{L}, \\ \theta &= \frac{T - T_i}{T_h - T_i}, & \theta_s &= \frac{T_s - T_i}{T_h - T_i} \end{aligned}$$

and the parameters Re , Ri , Pr and K are defined as

$$Re = \frac{u_i L}{\nu}, \quad Ri = \frac{g\beta(T - T_i)L}{u_i^2}, \quad Pr = \frac{\nu}{\alpha} \quad \text{and} \quad K = \frac{k_s}{k}.$$

The appropriate dimensionless form of the boundary conditions used to solve equations (1)–(5) inside the cavity are given as:

$$U = 1, \quad V = 0, \quad \theta = 0 \quad \text{at the inlet;}$$

$$P = 0 \quad \text{convective boundary condition (CBC) at the outlet;}$$

$$U = 0, \quad V = 0 \quad \text{at all solid boundaries;}$$

$$\theta = 1 \quad \text{at the heated right vertical wall;}$$

$$\left. \frac{\partial \theta}{\partial X} \right|_{X=0} = \left. \frac{\partial \theta}{\partial Y} \right|_{Y=1,0} \quad \text{at the left, top and bottom walls;}$$

$$\left(\frac{\partial \theta}{\partial x} \right)_{fluid} = K \left(\frac{\partial \theta_s}{\partial x} \right)_{solid} \quad \text{at the solid-fluid vertical interfaces of the block;}$$

$$\left(\frac{\partial \theta}{\partial Y} \right)_{fluid} = K \left(\frac{\partial \theta_s}{\partial Y} \right)_{solid} \quad \text{at the solid-fluid horizontal interfaces of the block.}$$

The average Nusselt number (Nu) at the hot wall is defined as

$$Nu = \frac{1}{L_h} \int_0^{L_h/L} \frac{\partial \theta}{\partial X} \Big|_{X=1} dY \quad (6)$$

and the bulk average temperature in the cavity is defined as

$$\theta_{av} = \int \frac{1}{\bar{V}} \theta d\bar{V}, \quad (7)$$

where $L_h = L - 0.1/L$ is the length of the hot wall and \bar{V} is the cavity volume.

4 Numerical technique

The numerical procedure used in this work is based on the Galerkin weighted residual method of finite element formulation. The application of this technique is well described by Taylor and Hood [13] and Dechaumphai [14]. In this method, the solution domain is discretized into finite element meshes, which are composed of non-uniform triangular elements. Then the nonlinear governing partial differential equations (i.e. mass, momentum and energy equations) are transferred into a system of integral equations by applying Galerkin weighted residual method. The integration involved in each term of these equations is performed by using Gauss quadrature method. The nonlinear algebraic equations so obtained are modified by imposition of boundary conditions. These modified nonlinear equations are transferred into linear algebraic equations by using Newton's method. Finally, these linear equations are solved by using Triangular Factorization method.

4.1 Grid refinement check

Five different grid sizes of 3976, 4798, 6158, 6278 and 7724 elements with 25555, 30619, 38973, 39870, and 48945 nodes respectively are chosen for the present simulation to test the independency of the results with the grid size variations. Average Nusselt number at the heated surface, average temperature of the fluid inside the cavity and the solution time are monitored at $Ri = 1.0$, $L_x = L_y = 0.5$, $D = 0.2$ and $K = 5.0$ for these grid elements as shown in Table 1.

Table 1. Grid sensitivity check at $Ri = 1.0$, $K = 5.0$, $D = 0.2$ and $L_x = L_y = 0.5$

Elements (Nodes)	3976 (25555)	4798 (30619)	6158 (38973)	6278 (39870)	7724 (48945)
Nu	4.8463	4.8478	4.8488	4.8489	4.8489
θ_{av}	0.1905	0.1905	0.1905	0.1905	0.1905
Time [s]	385.219	493.235	682.985	698.703	927.359

The magnitude of average Nusselt number at the heated surface and average temperature of the fluid inside the cavity for 39870 nodes with 6278 elements shows a very little difference with the results obtained for the other denser grids. Hence for the rest of the calculation in this study, a grid size of 39870 nodes with 6278 elements is chosen for better accuracy.

4.2 Code validation

For code validation tests, see Rahman et al. [12].

5 Results and discussion

A numerical study has been performed through finite element method to analyze the laminar mixed convection heat transfer and fluid flow in a vented square cavity filled with a horizontal square solid block. Effect of the parameters such as Richardson number (Ri), dimensionless block length (D), solid-fluid thermal conductivity ratio (K) and the location of the solid block (L_x, L_y) on heat transfer and fluid flow of the cavity have analyzed. We have presented the results in two sections. The first section has focused on flow and temperature fields, which contents streamlines and isotherms for the different cases. The following section has discussed heat transfer including average Nusselt numbers at the hot wall, average fluid temperature in the cavity and temperature at the block center. The range of Ri for this investigation has varied from 0.0 to 5.0 by changing Gr while keeping Re fixed at 100. Air is chosen as working fluid with $Pr = 0.71$.

5.1 Flow and temperature fields

Flow and temperature fields have simulated using streamlines and isotherms for the mentioned parameters. Effect of block size on streamlines and isotherms have presented in Figs. 2 and 3 for $K = 5.0$, $L_x = L_y = 0.5$ and various Ri (0.0, 1.0 and 5.0). The flow structure in the absence of free convection effect (i.e. $Ri = 0$) and for the four different values of D has shown in the left column of Fig. 2. At $Ri = 0.0$ and $D = 0.0$, it has been seen that a comparatively large uni-cellular vortex appears at the left top corner of the cavity and a very small vortex appears at the right bottom corner of the cavity, which are owing to the effect of buoyancy force. Further increase of D sharply decreases the size of the vortex. This is due to increasing the size of the block gives rise to a decrease in the space available for the buoyancy force induced vortex. For $Ri = 1.0$ and $D = 0.0$, it has been also seen from Fig. 2 that the natural convection effect is present, but remains relatively weak at high values of D , since the open lines characterizing the imposed flow are still dominant. Further increase of Ri to 5.0, gradually increase the size of the vortex for $D = 0.0$. This expansion of the size of the vortex squeezes the induced forced flow path resulting almost same kinetic energy in the bulk-induced flow as that of the inlet port. It must be noticed that in this case the size of the vortex reduced dramatically at the highest value of $D = 0.6$. The isotherms in the absence of block ($D = 0.0$) and for the three values of Ri are shown in the bottom row of Fig. 3.

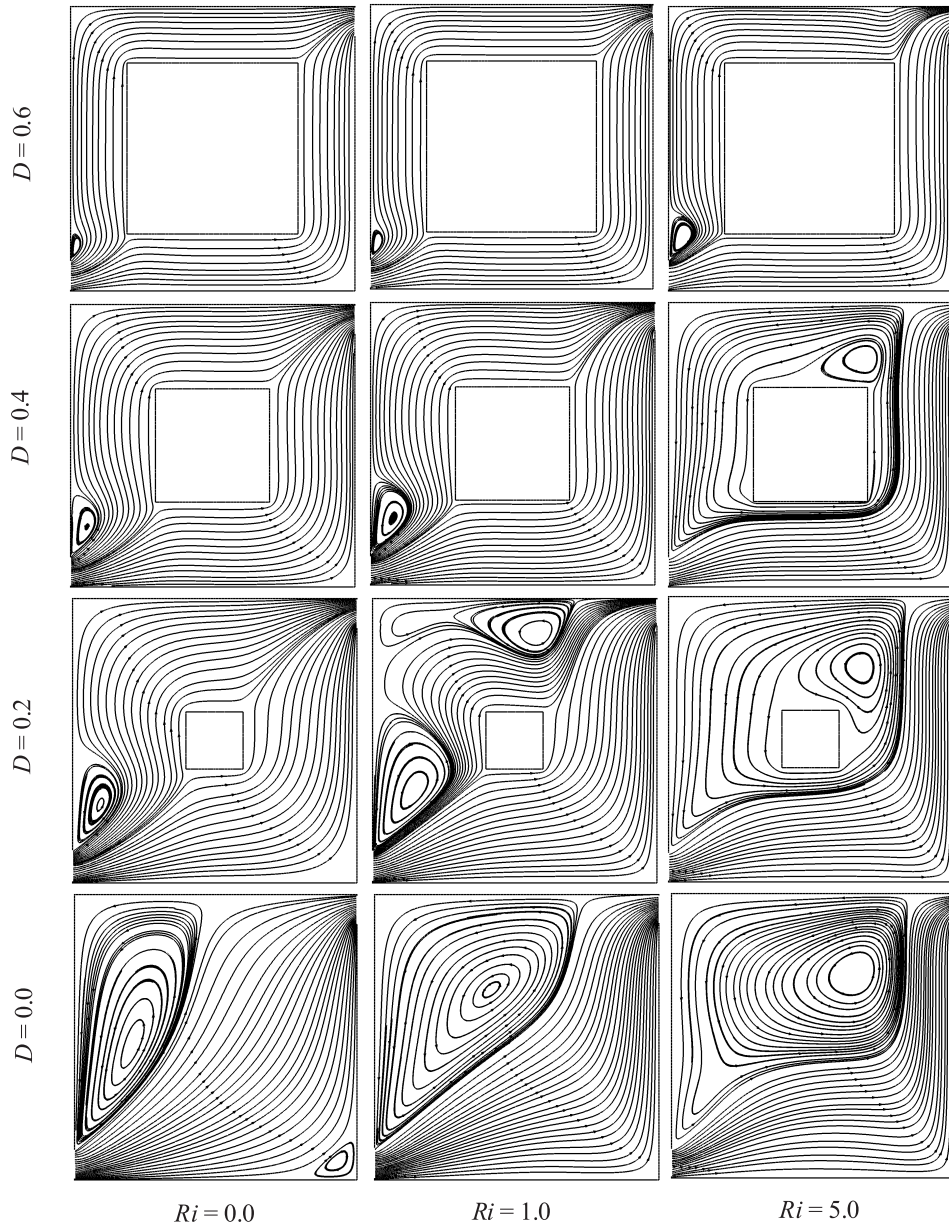


Fig. 2. Streamlines for different block length and Richardson numbers, while $L_x = L_y = 0.5$ and $K = 5.0$.

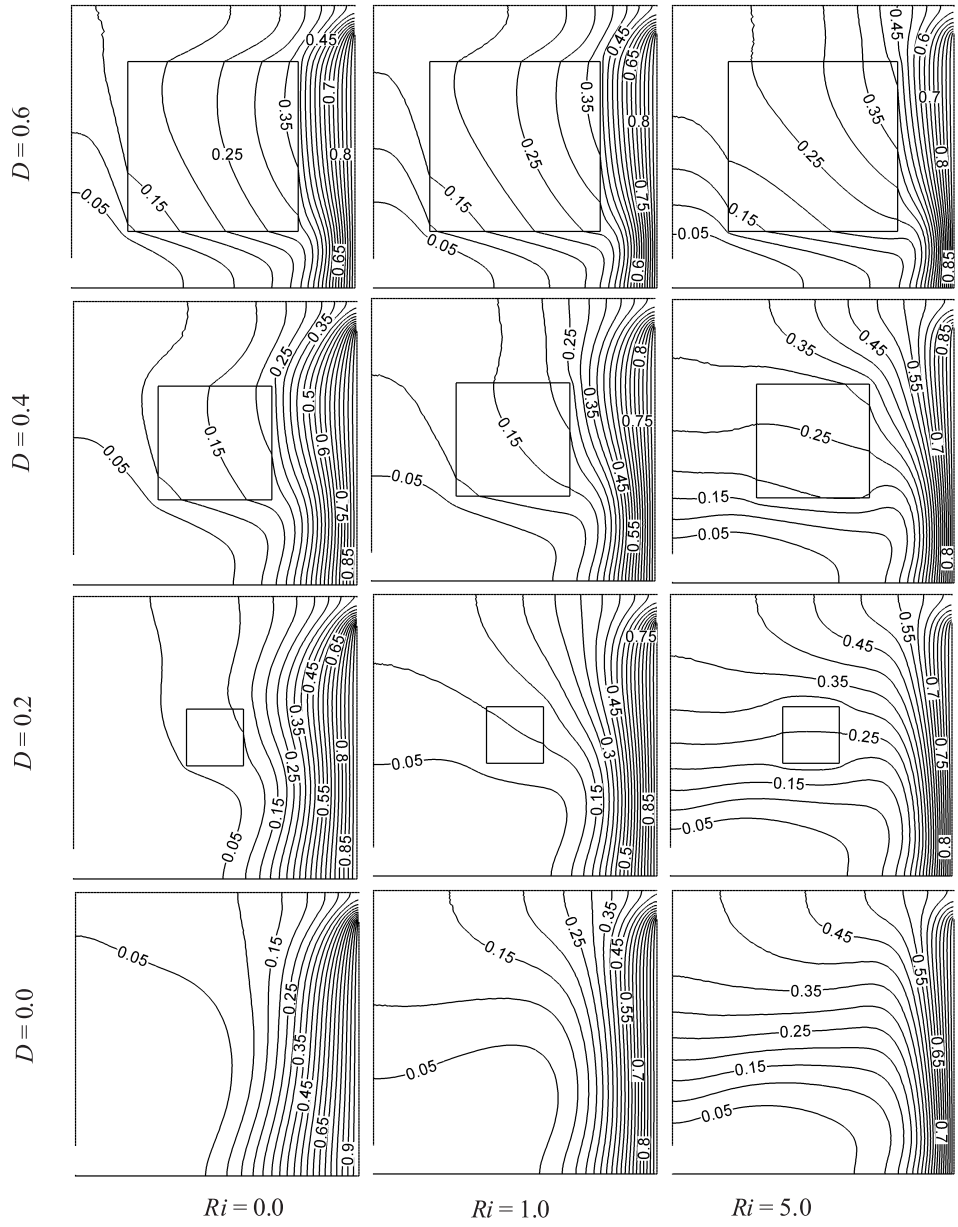


Fig. 3. Isotherms for different block length and Richardson numbers, while $L_x = L_y = 0.5$ and $K = 5.0$.

At $Ri = 0.0$ and $D = 0.0$, the high temperature region is concentrated near the hot wall and the isothermal lines are linear and parallel to the heated surface in the cavity, indicating conduction and forced convection dominant heat transfer. On the other hand, the concentrated temperature region become thin and the isothermal lines become nonlinear for $Ri = 1.0$ and various values of D . Further Ri increases to 5.0, the nonlinearity in the isotherms become higher and plume formation is profound, indicating the well established natural convection. As we compared the isothermal lines for $D = 0.2$ and various Ri with the isothermal lines for $D = 0.0$ and various Ri , only small difference in isotherms is observed. Further increasing the length of the block gives the higher nonlinearity in the isothermal lines of the cavity.

The effect of the solid-fluid thermal conductivity ratio (K) on streamlines and isotherms for $D = 0.2$ and $L_x = L_y = 0.5$ and various Ri have presented in Figs. 4 and 5 respectively. At $Ri = 0.0$ and $K = 0.2$, the bulk induced flow expands in the cavity resulting increase in potential energy. Here a small recirculation cell is formed just at the top of the inlet port of the cavity. The streamlines for the other cases (i.e. $K = 1.0, 5.0, 10.0$) at $Ri = 0.0$ are almost identical. Further as Ri increases, the vortex spreads. As a consequence, the induced flow is squeezed and the vortex covers the cavity, indicating the supremacy of natural convection in the cavity. Again at $Ri = 0.0$ and $K = 0.2$, the isothermal lines are almost parallel and concentrated to the hot surface as shown in Fig. 5. Making a comparison of the isothermal lines for $Ri = 0.0$ and various K , no significant difference is found except that the isothermal lines at higher K are shifted from the center of the block. As Ri increases for a permanent K , nonlinearity of the isotherms becomes higher and plume formation is philosophical, indicating the well established natural convection heat transfer.

The distribution of streamlines and isothermal lines for various locations of the square block at $Ri = 0.0, 1.0$ and 5.0, while $D = 0.2$ and $K = 5.0$ have shown in Figs. 6 and 7. When the inner block is placed at the center (0.25, 0.5) as shown in the bottom row of the Fig. 6, a bi-cellular vortex is seen just above the inlet port and occupies the left-top portion of the cavity and a pocket of fluid formed at the right bottom corner in the cavity for $Ri = 0.0$. Further at $Ri = 1.0$ the bi-cellular vortex spreads and the pocket of fluid the right bottom corner in the cavity is out. Also the flow changes its pattern from bi-cellular vortex to a uni-cellular vortex at $Ri = 5.0$. The corresponding isotherms for the lower values of Ri are uniformly distributed around the heat source, display that the heat is mainly transport by diffusion due to weak buoyancy flow. The distribution of isotherms in the cavity at $Ri = 5.0$ is significantly different from that at the lower values of Ri , because the buoyancy induced convection becomes more predominant than conduction. When the inner block moves closer to the heated surface along the mid-horizontal plane, the pattern of vortex located just above the inlet port in the cavity is also uni-cellular. The distribution of the isotherms for different Ri shows a similar pattern to the case, where block moves near the left wall along the mid-horizontal plane for different Ri . However, when the inner block moves closer to the bottom wall along the mid-vertical plane a very small uni-cellular vortex is formed just the top of the inlet at $Ri = 0.0$ and 1.0, but for $Ri = 5.0$, the flow pattern has changed drastically from a very small vortex into two large vortices and thereby squeezes the induced flow path due to the supremacy of natural

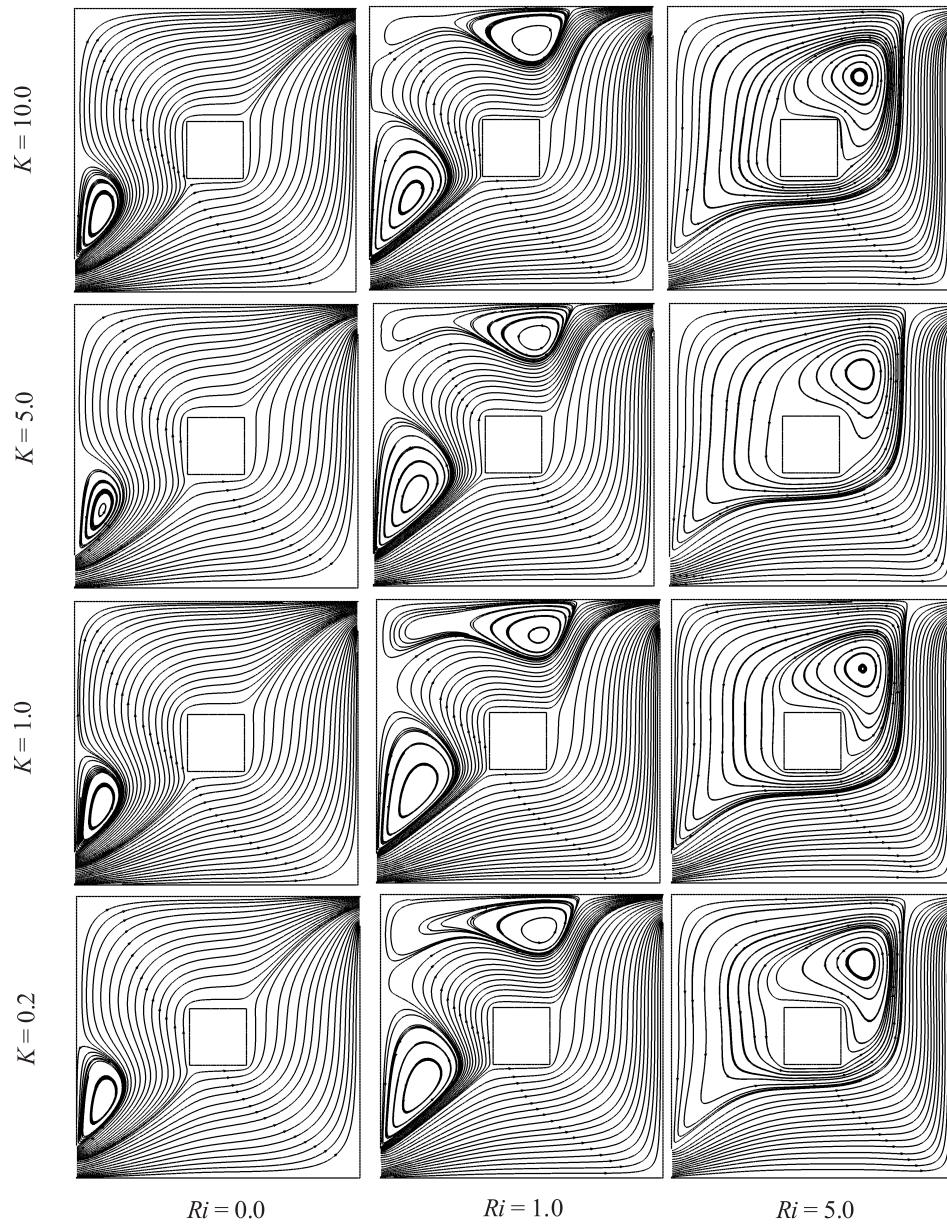


Fig. 4. Streamlines for different thermal conductivity ratios and Richardson numbers, while $L_x = L_y = 0.5$ and $D = 0.2$.

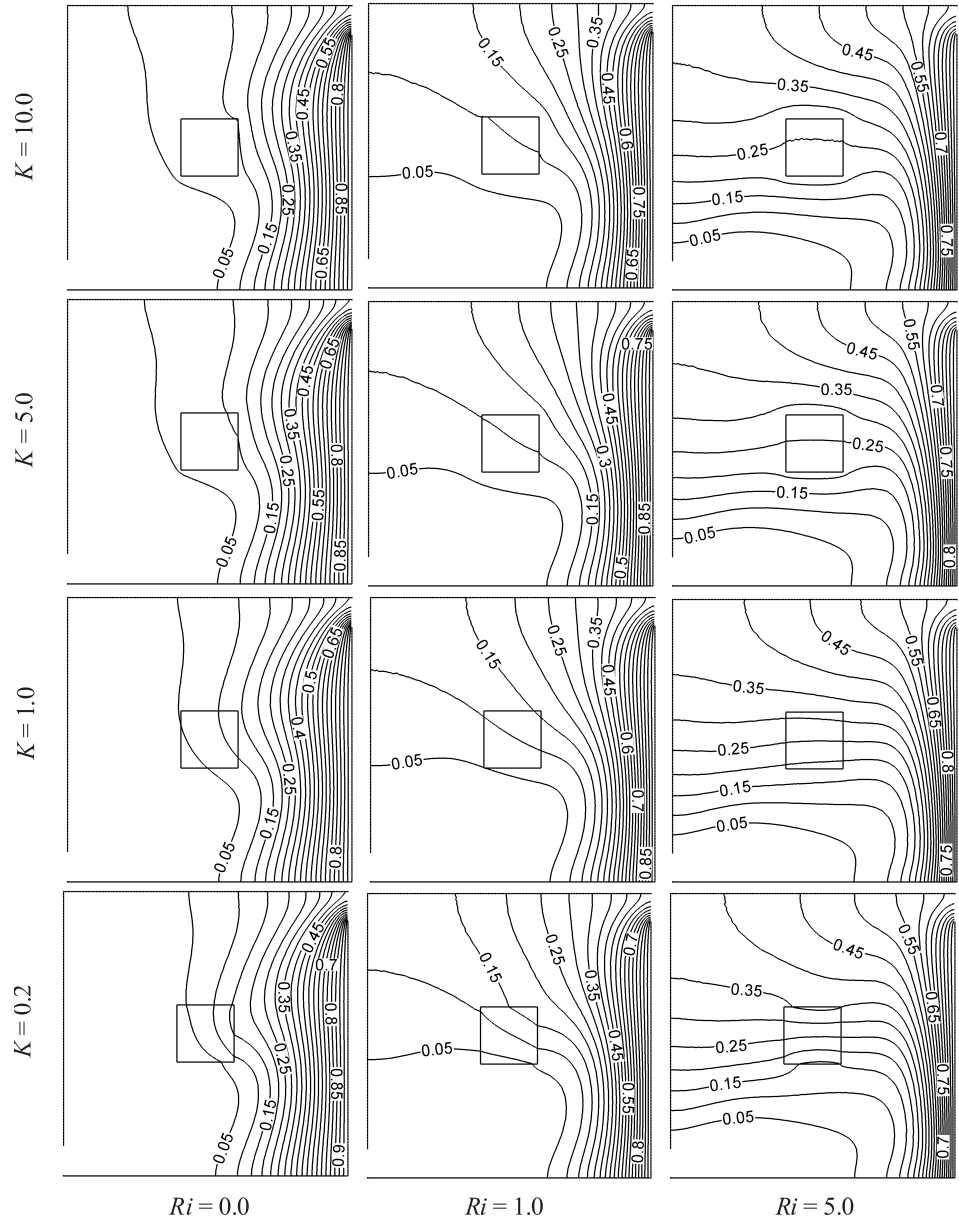


Fig. 5. Isotherms for different thermal conductivity ratios and Richardson numbers, while $L_x = L_y = 0.5$ and $D = 0.2$.

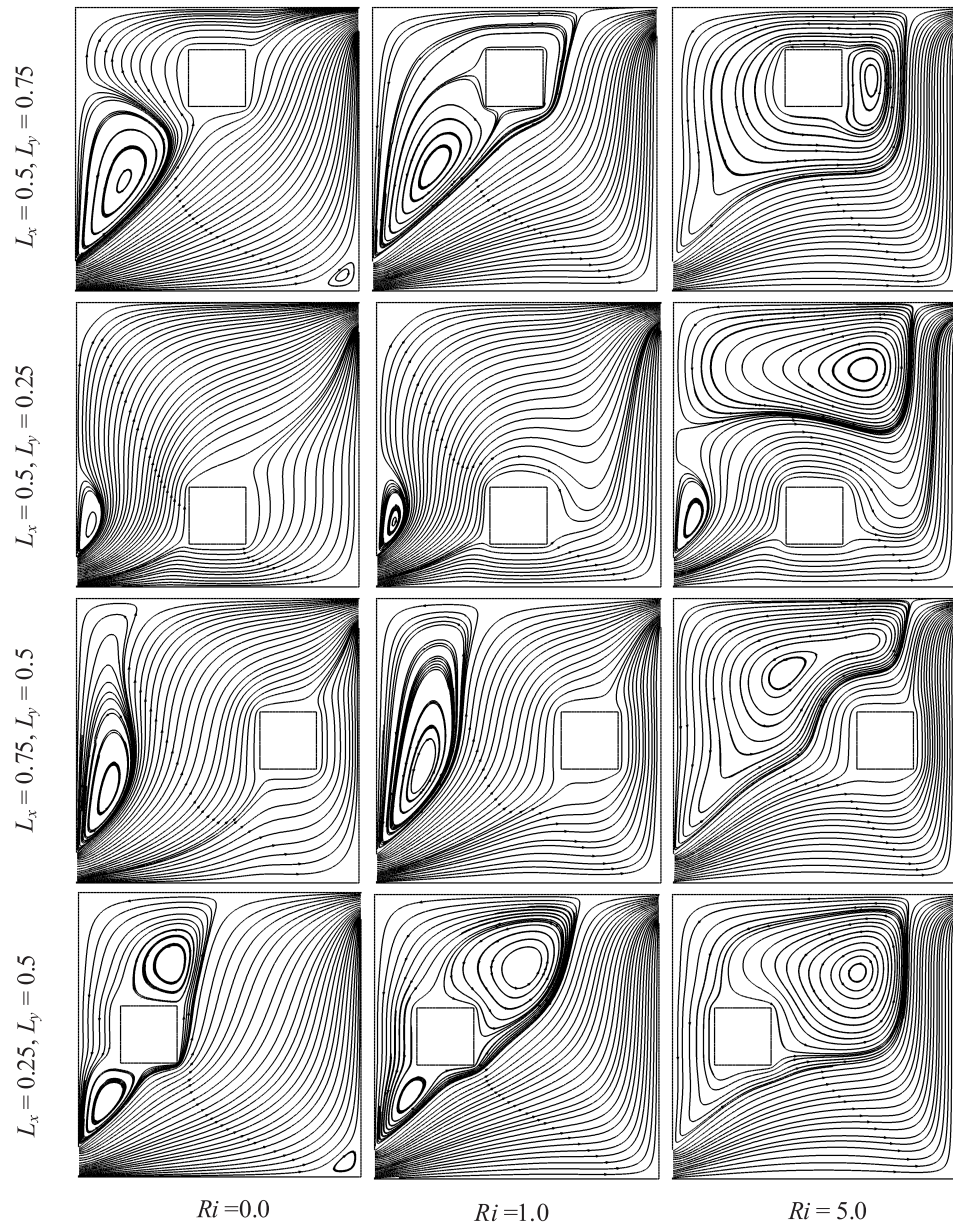


Fig. 6. Streamlines for different locations of the block and Richardson numbers, while $K = 5.0$ and $D = 0.2$.

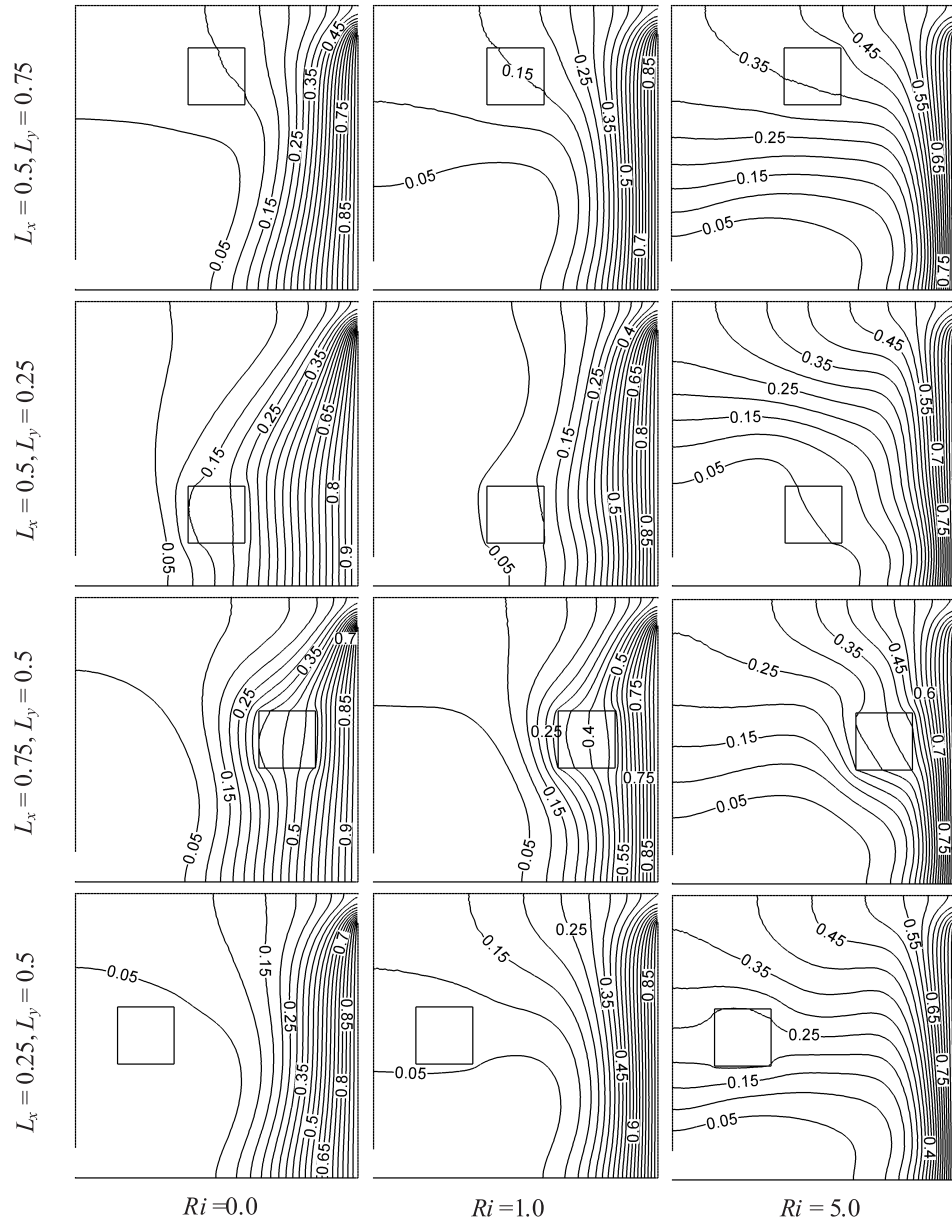


Fig. 7. Isotherms for different locations of the block and Richardson numbers while $K = 5.0$ and $D = 0.2$.

convection in the cavity. The isothermal lines in this case are more concentrated and vertical at the heat source for $Ri = 0.0, 1.0$, due to weak buoyancy flow. As Ri increases to 5.0, the isotherms become nonlinear and plume is formed which are the cryptogram of strong natural convection heat transfer. Also when the inner block moves closer to the top wall along the mid-vertical plane a uni-cellular vortex has formed just over the inlet port and occupies the left-top portion in the cavity and a pocket of fluid formed at the right bottom corner in the cavity for $Ri = 0.0$. Further increase of Ri gradually develops the size of the vortex, located at the left top corner of the cavity and diminishes the pocket of the fluid at the right bottom corner in the cavity. The isothermal lines surrounding the heat source seem to have no significant difference that of as the block moves closer to the left wall along the mid-vertical plane.

5.2 Heat transfer

Plots of the average Nusselt number (Nu) at the heated wall, average temperature (θ_{av}) of the fluid in the cavity and the dimensionless temperature (θ_c) at the block center as a function of Ri and D have shown in Fig. 8. As Ri increases, average Nusselt number (Nu) at the heated wall increases monotonically for all values of D , which is due to increasing Ri enhances convective heat transfer. On the other hand, for a particular values of Ri average Nusselt number (Nu) at the heated wall is the highest for $D = 0.6$ in the forced convection dominated region ($0.0 \leq Ri \leq 1.0$) and for $D = 0.4$ in the free convection dominated region. It has been seen that the average temperature (θ_{av}) of the fluid in the cavity and the temperature (θ_c) at the block center increase with increasing Ri for a particular values of D . On the other hand, the average temperature (θ_{av}) of the fluid in the cavity and the temperature (θ_c) at the block center increase with increasing D for a particular value of Ri . This can be attributed to the fact that a large centered square block narrows the regions available for both the warm and cold fluid flows.

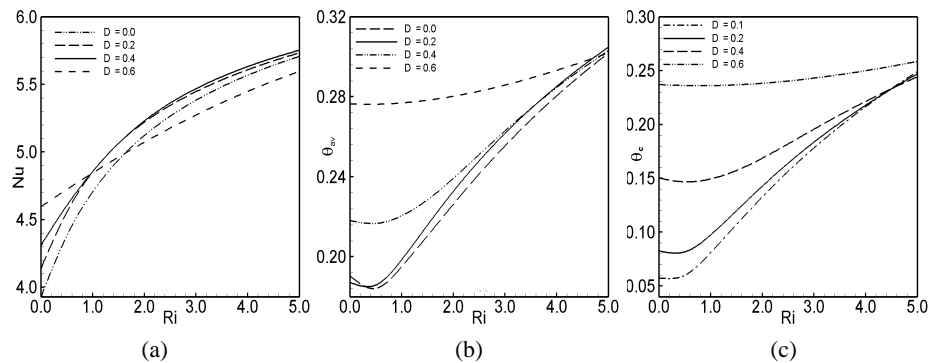


Fig. 8. Effect of block length on (a) average Nusselt number; (b) average fluid temperature and (c) temperature at the block center for various Ri , while $L_x = L_y = 0.5$ and $K = 5.0$.

The effect of Richardson number on the average Nusselt number (Nu) at the heated surface, average temperature of the fluid in the cavity and temperature at the block center for different solid-fluid thermal conductivity ratio has shown in Fig. 9. As Ri increases, average Nusselt number (Nu) at the hot surface sharply increases for all values of K . A careful observation on Fig. 9(a) shows that Nu is the highest for $K = 5.0$ and 10.0 at $Ri \leq 0.4$ and for $K = 1.0$ at $0.4 < Ri < 1.0$. Beyond these values of Ri it is the highest for $K = 0.2$. As Ri increases average temperature of the fluid and the temperature at the block center increases gradually for all values of K in the cavity. On the other hand, for a particular value of Ri the average temperature (θ_{av}) of the fluid in the cavity and the temperature (θ_c) at the block center is always the lowest for $K = 0.2$. This scenario occurs because the block with $K = 0.2$ acts as an insulator and prevents heat transfer between the hot and the cold fluid streams.

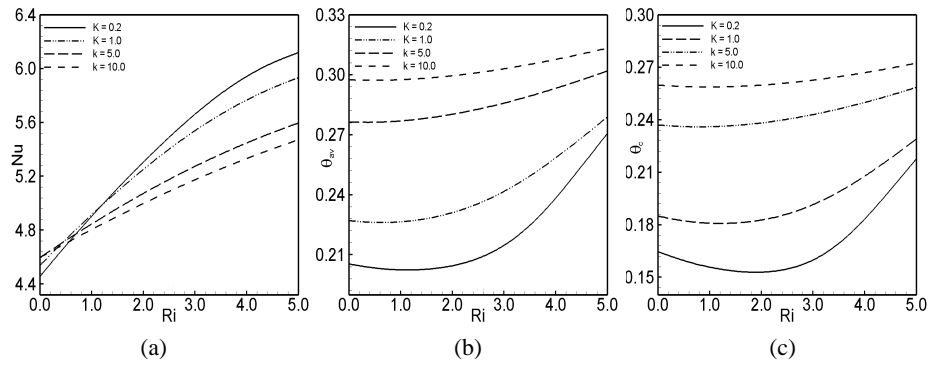


Fig. 9. Effect of thermal conductivity ratio on (a) average Nusselt number; (b) average fluid temperature and (c) temperature at the block center for various Ri , while $L_x = L_y = 0.5$ and $D = 0.6$.

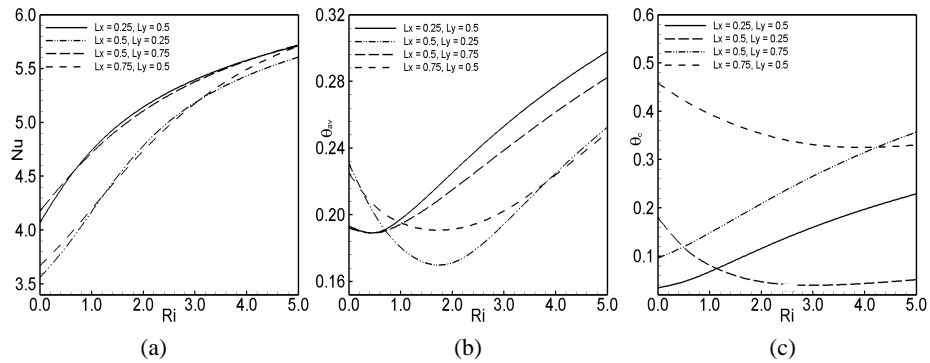


Fig. 10. Effect of the locations of the block on (a) average Nusselt number; (b) average fluid temperature and (c) temperature at the block center for various Ri , while $K = 5.0$ and $D = 0.2$.

The average Nusselt number (Nu) at the heated surface, the average temperature (θ_{av}) of the fluid and the temperature (θ_c) at the block center in the cavity are plotted against Richardson numbers and for the four different locations of the block have shown in Fig. 10. From these figures it has seen that the average Nusselt number smoothly increases with increasing Ri and the average temperature of the fluid and the temperature at the block center in the cavity are not monotonic with increasing Ri for different locations of the solid block.

6 Conclusion

A numerical investigation is made of laminar mixed-convective in a square cavity with a heat conducting horizontal square block. Results are obtained for wide ranges of parameters Richardson number (Ri), dimensionless block length (D), solid-fluid thermal conductivity ratio (K) and the location of the solid block (L_x, L_y).

In view of the obtained results, the following findings have been summarized:

- Block size affects strongly the streamline distribution in the cavity. As a result, buoyancy forced-induced circulation cell reduces with increasing block size. Comparatively small effect on the isotherms is observed for different block size. The average Nusselt number at the heated surface is the highest for the largest block length $D = 0.6$ in the forced convection dominated region and for the second largest length $D = 0.4$ in the free convection dominated region. On the other hand, a gradual increase in the heat transfer rate is found with increasing Ri at constant values of block length.
- Material properties (K) have insignificant effect on the flow field and have significant effect on the thermal fields. An unexpected result is found for the dependence of thermal transport on the solid-fluid thermal conductivity ratio. For somewhat large solid block an obvious enhancement in the heat transfer is obtained for the largest values of K in the forced convection dominated region and for the lowest value of K in the free convection dominated region. However, a steady increase in the heat transfer rate is found with increasing Ri at constant values of K .
- Locations of the block have significant effect on the flow and thermal fields. The value of average Nusselt number is the highest in the forced convection dominated area when the block is located near the top wall along the mid-vertical plane and in the free convection dominated area when the block moves closure to the left vertical wall along the mid-horizontal plane. On the other hand, a gradual increase in the heat transfer rate has found with increasing Ri at constant values of block length. The values of θ_{av} and θ_c are not monotonic with increasing values of Ri for different locations of the block.

References

1. M. K. Das, K. S. K. Reddy, Conjugate natural convection heat transfer in an inclined square cavity containing a conducting block, *Int. J. Heat Mass Tran.*, **49**, pp. 4987–5000, 2006.

2. F. Y. Zhao, G. F. Tang, D. Lin, Conjugate natural convection in enclosures with external and internal heat sources, *Int. J. Eng. Sci.*, **44**, pp. 148–165, 2006.
3. F. Xu, J. C. Patterson, C. Lei, Experimental observations of the thermal flow around a square obstruction on a vertical wall in a differentially heated cavity, *Exp. Fluids*, **40**, pp. 364–371, 2006.
4. M. T. Bhoite, G. S. V. L. Narasimham, M. V. K. Murthy, Mixed convection in a shallow enclosure with a series of heat generating components, *Int. J. Therm. Sci.*, **44**, pp. 125–135, 2005.
5. E. J. Braga, M. J. S. de Lemos, Laminar natural convection in cavities filled with circular and square rods, *Int. Commun. Heat Mass*, **32**, pp. 1289–1297, 2005.
6. S. H. Tashim, M. R. Collins, Suppressing natural convection in a differentially heated square cavity with an arc shaped baffle, *Int. Commun. Heat Mass*, **32**, pp. 94–106, 2005.
7. E. Bilgen, T. Yamane, Conjugate heat transfer in enclosures with openings for ventilation, *Heat Mass Transfer*, **40**, pp. 401–411, 2004.
8. S. F. Dong, Y. T. Li, Conjugate of natural convection and conduction in a complicated enclosure, *Int. J. Heat Mass Tran.*, **47**, pp. 2233–2239, 2004.
9. D. G. Roychowdhury, S. K. Das, T. S. Sundararajan, Numerical simulation of natural convection heat transfer and fluid flow around a heated cylinder inside an enclosure, *Heat Mass Transfer*, **38**, pp. 565–576, 2002.
10. J. M. House, C. Beckermann, T. F. Smith, Effect of a centered conducting body on natural convection heat transfer in an enclosure, *Numerical Heat Tr. A-Appl.*, **18**, pp. 213–225, 1990.
11. J. Y. Oh, M. Y. Ha, K. C. Kim, Numerical study of heat transfer and flow of natural convection in an enclosure with a heat generating conducting body, *Numerical Heat Tr. A-Appl.*, **31**, pp. 289–304, 1997.
12. M. M. Rahman, M. A. Alim, M. A. H. Mamun, Finite element analysis of mixed convection in a rectangular cavity with a heat-conducting horizontal circular cylinder, *Nonlinear Anal. Model. Control*, **14**(2), pp. 217–247, 2009.
13. C. Taylor, P. Hood, A numerical solution of the Navier-Stokes equations using finite element technique, I, *Computer and Fluids*, **1**, pp. 73–89, 1973.
14. P. Dechaumphai, *Finite Element Method in Engineering*, 2nd ed., Chulalongkorn University Press, Bangkok, 1999.